CHAPTER 2

BASIN CREATION AND SOURCE TERRAINS

Here we explore the tectonic processes that create sedimentary basins and their source terrains. These tectonic processes are rarely observed directly, but rather are interpreted from the geologic record after excluding such variables as climate. Such a post mortem requires that a basin be preserved. Thus, there not only must be processes that create a basin, but also processes that preserve it as part of the geologic record. Virtually all basins eventually meet their demise through either tectonic activity or removal by the processes that created them. The positive side to this life cycle is that we can observe both the development and removal stages of a basin and obtain insight into physical processes in the Earth's crust and upper mantle. Sedimentary basins thus provide a telescope for looking deep into the Earth.

ISOSTASY AND ACCOMMODATION SPACE

A sedimentary basin is a region of "accommodation space" at the earth's surface. Accommodation space is the volume, or in the vertical plane, the area between the land surface or sea bed and the local base level. Without accommodation space, sediment only accumulates temporarily before it is removed by erosion and transported elsewhere. Accommodation space can be formed by several processes. It can be formed by folding or faulting that produces a local depression. More commonly, accommodation space in long-lived basins results from mass loading on the Earth's lithosphere. These basins can be large in areal extent and span a long period of subsidence and deposition, as well as a long post-depositional existence. As we shall see, although the mass of sediment deposited in a basin will cause additional subsidence, deposition of sediment by itself cannot generate its own basin.

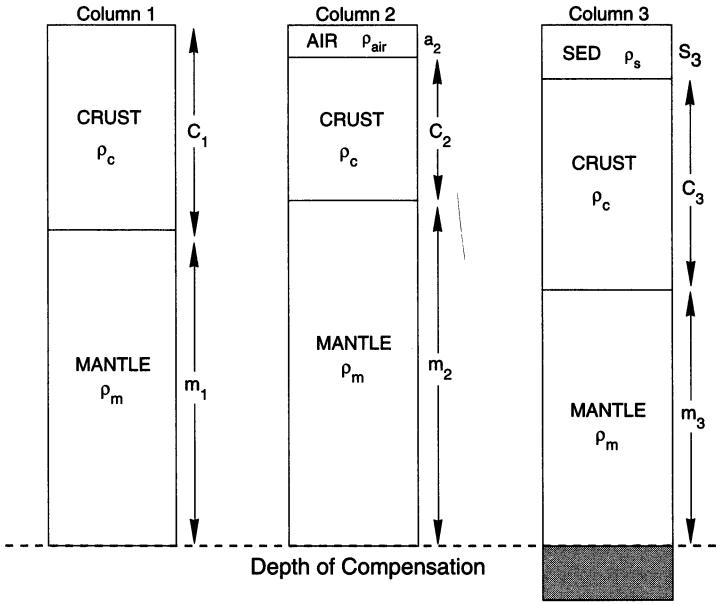

Figure 2-1 Standard columns to determine isostatic equilibrium as a function of crustal thickness. Mass in columns must be equal, implying changes in relative heights of mantle, air, water, and sediment layers.

The role of isostasy in the generation of mountains and basins has long been recognized. Isostatic balance is used to relate the height of mountains to crustal thickness, with Pratt's and Airy's models as explanations of gravity anomalies and heights associated with mountain chains. Although isostatic models differ, common to each is the concept that at a particular depth within the Earth, termed the depth of compensation, there is an equal pressure resulting from the mass of crust above this depth. Although the depth of compensation can be viewed variously in analyzing sedimentary basins, we can generalize that the compensation depth lies within the asthenospheric mantle. This generalization allows a variety of supracrustal and intracrustal processes that affect isostatic balance to be included.

By nature, isostasy is a one-dimensional process. Mass in the lithosphere is described by a series of vertical columns of specified density and depth that do not interact with each other. Figure 2-1 shows two columns in isostatic equilibrium, implying that the pressure at the base of the two columns is equal, or alternatively, that the integrated mass in each column in the presence of gravity is equal. Column 1 of Figure 2-1 shows a simple lithospheric system composed of crust of density ρ_c and thickness c_1, and a mantle of density ρ_m and thickness m_1. Column 1 can serve as a reference column for isostatic calculations. Column 2 is more complex, having three layers consisting of crust of density ρ_c and thickness c_2, mantle of density ρ_m and thickness m_2, and a third layer consisting of air with density ρ_{air} (zero for our purposes) and thickness a_2. This is the Airy model that assumes constant density among columns for the crust or mantle layers. By contrast, in the Pratt model, the density of the crustal layer can vary among the columns.

The isostatic equilibrium of columns 1 and 2 in Figure 2-1 can be described by equating their weight (mass x gravity):

$$(\rho_c c_1 + \rho_m m_1)\, g = (\rho_c c_2 + \rho_m m_2 + \rho_{air} a_2)\, g \qquad \textbf{(2-1)}$$

Here the total column thickness (from the surface to the depth of compensation) must be the same for both columns, or

$$c_1 + m_1 = c_2 + m_2 + a_2 \quad \text{(2-2)}$$

To investigate these equivalencies, let us compare two regions with different crustal thicknesses. In Figure 2-1 we want to evaluate the difference in surface elevation between columns one and two. This difference is expressed by a_2, the thickness of the column of air above the surface. An application might involve determining the initial accommodation space for a region of thinned crust, or equivalently, the rise in elevation of a region of thickened crust. To quantify the discussion we assume that the total thickness c_1 of the crust in column 1 is 35 km, and the thickness m_1 of the underlying lithospheric mantle is 65 km. This results in a total thickness for column 1 of 100 km, with the top of the column serving as the datum. The total thickness of column 2 is also 100 km, but we assume that the crust thickness c_2 is only 30 km. The resulting 70 km of available material is either mantle m_2 or air a_2. Thus the sum $m_2 + a_2$ is 70 km. We can assume typical densities for the layers, with ρ_c = 2700 kg m^{-3}, ρ_m = 3300 kg m^{-3}, and ρ_{air} = 0 kg m^{-3}. Inserting in (2-1) gives us:

$$\rho_c(35)\,g + \rho_m(65)\,g = \rho_c(30)\,g + \rho_m(70 - a_2)\,g \quad \text{(2-3)}$$

The acceleration of gravity g cancels on both sides, yielding:

$$\rho_c(35 - 30) = \rho_m[(70 - a_2) - 65] \quad \text{(2-4)}$$

which reduces to:

$$\rho_c(5) = \rho_m(5 - a_2) \quad \text{(2-5)}$$

and finally to:

$$a_2 = 5\left(1 - \frac{\rho_c}{\rho_m}\right) \quad \text{(2-6)}$$

The above densities yield about 0.9 km for a_2. Thus a change of 5 km in crustal thickness results in a change in elevation of slightly less than 1 km.

This example is the simplest form of isostatic balance. We can add complications by assuming that accommodation space created by subsidence associated with crustal thinning is filled by either water or sediment. For either, the last term on the right-hand side of (2-1) is replaced by equivalent terms for sediment (ρ_s, s_2) or water (ρ_w, w_2). Equation (2-3) then becomes:

$$\rho_c(35)\,g + \rho_m(65)\,g = \rho_c(30)\,g + \rho_m(70 - w_2)\,g + \rho_w w_2 \quad \text{(2-7)}$$

The equivalent to (2-6) is:

$$w_2 = 5\frac{(\rho_m - \rho_c)}{(\rho_m - \rho_w)} \quad \text{(2-8)}$$

For an assumed density of water ρ_w of 1000 kg m^{-3}, w_2 is 1.3 km, and if the space is filled with sediment, ρ_s is 2000 kg m^{-3}, and s_2 is approximately 2.3 km.

In this example, we see that thinning the crust from 35 km to 30 km creates slightly less than 1 km of accommodation space. If the space is filled initially with water, it will deepen to approximately 1.3 km. The final thickness of sediment that can fill this space under conditions of isostatic equilibrium is 2.3 km.

To appreciate the importance of a process that produces accommodation space such as crustal thinning, we can investigate the effect of depositing 2.3 km of sediment on the Earth's surface. Because isostasy must be maintained, we can incorporate a third column (column 3 of Figure 2-1) that resembles our standard column in that crustal thickness is constant, with $c_1 = c_3$, but mass added in the sedimentary load will result in a smaller thickness of the mantle layer ($m_3 < m_1$). In this example, we no longer maintain the total column thickness of 100 km. The depth of compensation remains at the same depth (relative to our datum at the top of column 1), but the top of the sediment pile will extend above that by the amount that the total thickness of column 3 exceeds the thickness of column 1. The equivalent form of (2-1) is then:

$$(\rho_c c_1 + \rho_m m_1)\, g = (\rho_c c_3 + \rho_m m_3 + \rho_s s_3)\, g \tag{2-9}$$

which yields the following equation with relationships for column 3 and column 1 used:

$$(\rho_c 35 + \rho_m 65)\, g = (\rho_c 35 + \rho_m (65 - x) + \rho_s 2.3)\, g \tag{2-10}$$

Here we want to solve for x, which is the decrease in that part of the lithospheric column represented by the mantle. The crustal terms and g are equivalent on both sides of the equation, leaving

$$\rho_m 65 = \rho_m (65 - x) + \rho_s 2.3 \tag{2-11}$$

which becomes

$$\rho_m x = \rho_s 2.3 \tag{2-12}$$

or

$$x = \frac{\rho_s}{\rho_m} 2.3 \tag{2-13}$$

For the densities of sediment and mantle selected, x = 1.4 km. The mantle layer of column 3 is thus about 63.6 km in thickness, and column 3's total thickness is (s_3 + c_3 + m_3), which is about 100.9 km. Thus, the topography that results from depositing 2.3 km of sediment on the Earth's surface is equivalent to the accommodation space necessary to create a basin filled with sediment 2.3 km thick.

In discussing isostasy and creation of accommodation space, we touched on the one-dimensional nature of isostasy, which allows columns to be equated in a simple way but has limited application to actual basins. Only in broad basins is the concept of isostasy valid. The breadth of a basin necessary for us to use isostatic assumptions will be determined when we discuss flexure below. In general though, simple isostatic assumptions provide only a first approximation to the subsidence response of the lithosphere and the creation of accommodation space.

ISOSTASY AND BACKSTRIPPING

Isostatic assumptions are important in basin subsidence histories and in development of "geohistory" diagrams. Basin subsidence histories are usually based on stratigraphic columns or borehole logs, and as such are readily analyzable with isostatic models. A primary goal of "backstripping" in such an analysis is to determine the manner in which the basin would have subsided if sediments had not been deposited, thereby permitting us to decide among different hypotheses of basin formation. Backstripping determines the rate and magnitude of the creation

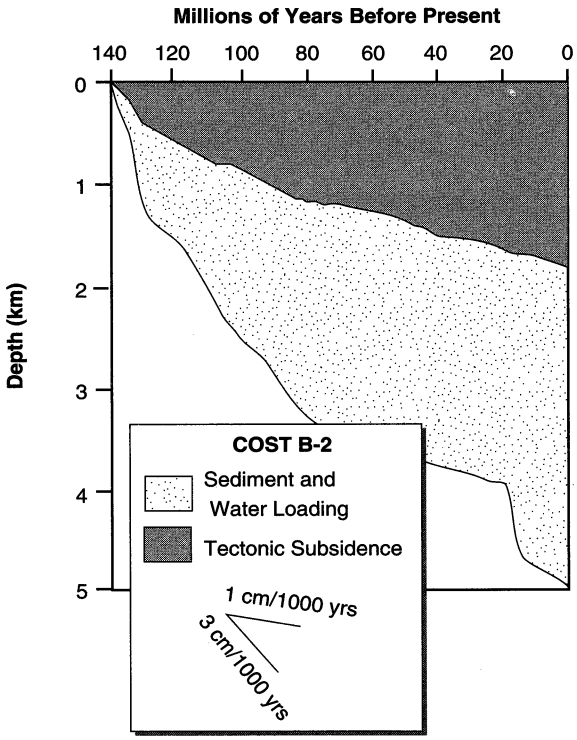

Figure 2-2
Geohistory diagram showing burial history of a stratigraphic horizon in COST B-2 well, Atlantic passive margin of eastern United States. Geohistory diagrams are often used to distinguish subsidence resulting from sediment loading from that due to tectonic subsidence (from Watts, 1981).

of accommodation space, independent of the sediment supply. Backstripping results are often shown in geohistory diagrams similar to Figure 2-2. While such diagrams are helpful, it is important to remember that they normally include the assumption of local isostatic compensation. If that assumption is invalid, the interpreted backstripping history may be flawed, as will be apparent in the discussion of flexural subsidence that follows.

LITHOSPHERIC FLEXURE

The manner in which the lithosphere deforms under a load is reflected in the geometry of sedimentary basins. When supracrustal loads are applied, as in overthrust terrains, the developing foreland basin is deepest adjacent to the load and usually shallows across the basin to a region of relative uplift accompanied by erosion. In rift basins, the depositional center is usually restricted to the interior of the rifted region. In passive margin basins, an offshore depositional center thins landward to a region of uplift and possibly erosion. Such basin geometries (with the possible exception of rift basins) are not compatible with the simple model of isostatic subsidence described previously. If we assume isostasy, the addition of a load, such as a thrust sheet, results in subsidence only immediately below the load and does not allow a basin to form except to the degree that depressions may form between folds or thrust sheets. Thus, the existence of other types of basins argues that we must look beyond isostasy to understand the development of accommodation space.

The fact that basins extend significantly beyond the loading mass implies that the lithosphere has mechanical strength that allows the load to be supported broadly by the lithosphere. Such behavior can be described as flexure. In fact, the response of the lithosphere should always be considered from a flexural stand-

point. Where broad loads are applied to the lithosphere, the flexural response is equivalent to the isostatic response described above, so that isostasy is an end-member case of flexure.

Here we will consider the lithosphere to be an elastic body, but flexure also can be described by more complex rheological models that include viscous and plastic deformation, in addition to elastic response. We derive the equations that describe elastic flexure of the lithosphere, evaluate the elastic properties of the lithosphere, and develop a model that allows us to simulate any load distribution. Such a model can describe the creation of accommodation space and the subsequent subsidence history of basins.

The Lithosphere as an Elastic Beam

In standard plate-tectonic models, the Earth's lithosphere is the rigid outer layer of the earth that supports significant stress over geologic time. This ability to support a finite level of stress, albeit with associated elastic strain, allows the lithosphere to deform in elastic flexure when an external load is applied (Turcotte and Schubert, 1982). Rather than repeat Turcotte and Schubert's entire derivation, we will extract material most relevant to basin development.

The concept of elastic flexure is illustrated when we cross a stream on a fallen log. Our weight on the log is a load that causes flexure of an elastic beam, the log. When the load is removed from the beam, the log returns to its original shape. In this way, elastic deformation is recoverable. However, when we deal with the lithosphere as an elastic beam or elastic plate, we must modify the fallen-log analogy. Unlike the log, the lithosphere rests on a substratum, the asthenosphere, that can support the beam and thus reduce its downward flexure when a load is applied. Therefore,we start with the basic equations of elastic flexure and later modify them to incorporate complications of the combined lithosphere and asthenosphere.

After application of a load to an elastic beam or plate, the beam or plate deforms until its geometry is in equilibrium under the forces and torques acting on it. A schematic view is given in Figure 2-3. A beam in equilibrium with the forces and torques applied to it implies that on any small section of the beam, the torques and forces are balanced. This permits us to derive the basic differential equation that describes elastic flexure. Figure 2-4 shows forces and torques acting on a

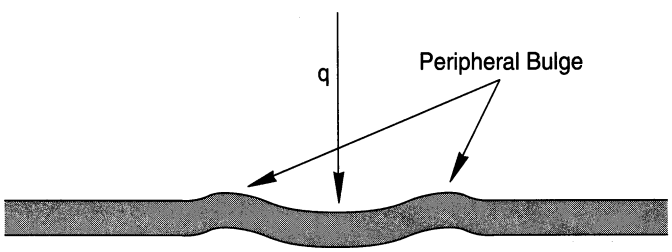

Figure 2-3 Flexure resulting from load applied to elastic beam.

small section of the beam. The force balance in the vertical direction on the small element is

$$q(x)\,dx + dV = 0 \tag{2-14}$$

where: $q(x)$ = downward force per unit area,
V = net shear force that acts on cross section of plate in vertical direction.

Equation (2-14) states that the net shear force acting downward across the top of the small beam segment is balanced by forces acting on the ends of the segment. In differential form this can be written as

$$\frac{dV}{dx} = -q(x) \tag{2-15}$$

Also acting on the beam segment are moments M and $M+dM$, which combine to give a net torque dM on the segment. Additionally, there are horizontal forces P on the segment that act with a net lever arm length of dw to produce a torque of $-Pdw$. Similarly, the forces (described generally by V) acting on the ends of the segment generate a torque Vdx acting on the segment. For the beam segment to be in equilibrium, these torques must also balance:

$$dM - Pdw = Vdx \tag{2-16}$$

This is equivalent (in differential form) to

$$\frac{dM}{dx} = V + P\frac{dw}{dx} \tag{2-17}$$

We can describe shear force V in terms of the downward force $q(x)$, by differentiating (2-17) with respect to x, and substituting (2-15), leading to

$$\frac{d^2M}{dx^2} = -q(x) + P\frac{d^2w}{dx^2} \tag{2-18}$$

Equation (2-18) describes deflection w in terms of both load $q(x)$ and bending moment M. If M can be described in terms of either w or $q(x)$, then we have the equation we seek. By implementing the elastic relationships between stress and

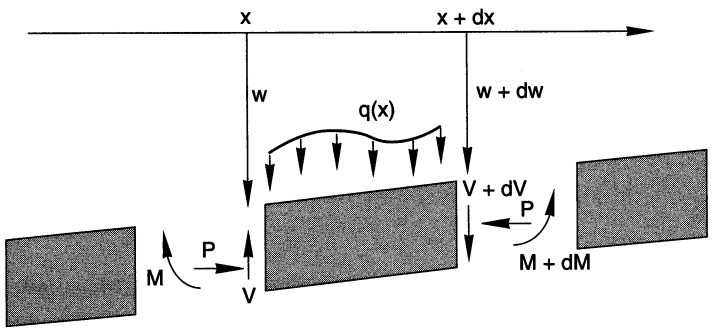

Figure 2-4 Forces and torques acting on element of elastic beam. In elastic equilibrium, all forces and torques balance.

strain, bending moment M can be related to curvature of the beam (the second derivative of deflection w with respect to x) and to the appropriate elastic properties of the beam, such that

$$M = -D\frac{d^2w}{dx^2} \tag{2-19}$$

Parameter D is the flexural rigidity, a measure of elastic strength of the beam given by

$$D = \frac{Eh^3}{12(1-\nu^2)} \tag{2-20}$$

where: E = Young's modulus,
ν = Poisson's ratio,
h = elastic thickness of beam.

Later, we will return to the importance of h, the elastic thickness. Substituting (2-19) in (2-18) yields the general equation for deflection of an elastic beam under an applied load:

$$D\frac{d^4w}{dx^4} = q(x) - P\frac{d^2w}{dx^2} \tag{2-21}$$

Equation (2-21) is the basis for our discussion of the elastic deformation of the lithosphere. We must solve this differential equation, subject to assumed boundary conditions, to simulate the behavior of the crust in the development of sedimentary basins.

Lithospheric Conditions

In solving (2-21), boundary conditions must be applied that best simulate the properties and geometries of the combined crustal and lithospheric system. We must determine the best way to represent the actual lithosphere within the confines of the model. The two characteristics of the plate that have the largest effect are its continuity and its elastic properties.

Of major importance is the decision whether the lithosphere is better represented as a continuous or broken plate. In a continuous-plate formulation, the applied load, such as mountain loads or basin fill, are assumed to be applied to the lithosphere at locations far from the ends of the plate. This condition is usually incorporated in most simulations of basin evolution, and as we shall see, it leads to a straightforward modeling algorithm. By contrast, the broken-plate formulation is appropriate where the loads are applied near the end of a plate, or over a fundamental zone of weakness in the lithosphere. The choice of continuous or broken lithosphere leads to somewhat different formulations of the modeling programs.

The material property by which we parameterize the flexural behavior of the lithosphere is the flexural rigidity D in (2-20). Of the terms that describe flexural rigidity, both Young's modulus E and Poisson's ratio ν vary relatively slightly with rock type or crustal composition. Typical values are 0.25 for ν and 70 GPa (Gigapascals) for E. Parameter h, which describes the elastic thickness of the plate, is dominant in controlling flexural rigidity and consequently the flexural behavior of the modeled lithosphere. There are two principle procedures for determining an appropriate value for h, and consequently for flexural rigidity D.

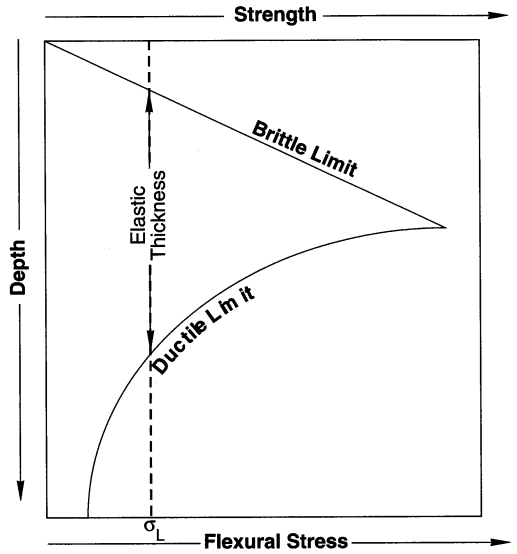

Figure 2-5
Diagram showing strength envelope of lithosphere as function of depth. If stresses acting on lithosphere exceed strength envelope, deformation occurs by brittle or ductile processes. Elastic thickness of lithosphere is given by region where stresses fall within elastic limit. σ_L is magnitude of stress in lithosphere induced by flexure.

A direct method for estimating h is to determine the thickness of the lithosphere in accordance with temperature and stress conditions that allow elastic behavior over geologic time scales. Most geologic materials behave elastically on geologic time scales of a million years or longer, provided that temperatures and stresses are within certain bounds. This approach involves characterizing the deformational behavior of the lithosphere through the use of strength envelopes (Figure 2-5). With strength envelopes, the elastic thickness is determined by that part of the lithosphere where the bending stresses generated by flexure are within the region which deforms elastically (Figure 2-5). Alternatively, studies of sedimentary basins, oceanic lithospheres, and continental interiors have led to a simpler definition of elastic thickness based primarily on the temperature distribution within the lithosphere. Combined temperature and structure models have shown that the 450 °C isotherm in the lithosphere is a reasonable marker for the base of the elastic lithosphere. Both strength-envelope and temperature-structure models give comparable elastic thicknesses, but because of its simplicity, the temperature-structure model is most often used in flexural studies.

Typical values for elastic thickness of the continental lithosphere range between 5 and 100 km. Lower elastic thicknesses occur in regions of very high heat flow and high crustal temperatures, as in the Basin and Range Province of the western United States and in rift regions. Values between 50 and 100 km occur in cooler, older, more stable regions, such as the shields and cratons. Elastic thicknesses of ~5 and ~55 km yield flexural rigidities D of 10^{21} Nm (Newton-meters) and 10^{24} Nm, respectively.

Flexure of a Continuous Plate

We now present methods and algorithms for flexure of a continuous plate. Flexural models typically assume that loads are line loads that are infinitely narrow, and that basin depressions are filled with sediment at all times. These assumptions, described in detail by Turcotte and Schubert (1982), provide a good starting approximation for general basin development. But we wish to incorporate erosion, sediment transport, and basin filling, and therefore we need loads of finite width,

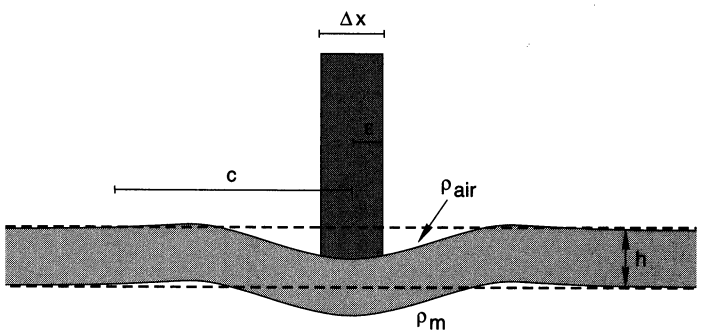

Figure 2-6 Diagram showing geometry of Green's-function load used in flexure-model formulation. Parameters used in Equations 2-22 and 2-23 are shown.

and flexural depressions that can be filled with sediment employing algorithms presented later.

Our approach is to discretize loads into finite-width elements of specified width, height, and density. We could solve (2-21) directly for the distributed load, but this would provide a complicated and non-general solution. It is better to solve (2-21) for a simple unit load of width Δx, unit height, and standard density. This unit load then can be scaled to simulate loads of differing height and density, and shifted to simulate the spatial pattern of actual loads. We can sum the flexure produced by each shifted, scaled unit load to obtain the total flexure.

This technique takes advantage of a well-known analytic approach using Green's function, named after George Green, a self-taught, eighteenth century English mathematician whose memoir that introduced his function was practically unknown until Lord Kelvin had it reprinted in 1846. Scaling, shifting, and adding the unit loads is termed a convolution. We use a Green's-function convolution because it is efficient for treating complex load and basin-fill geometries.

The Green's-function solution of (2-21) for a continuous plate with a finite-width load is given by two equations. One is applicable underneath the rectangular load, and the other applies to regions to the right or left of the load. The configuration of the Green's-function model is shown in Figure 2-6, and the solution for the node beneath the unit load is:

$$w = -\frac{K}{2}\left(2 - 2exp\left[-\frac{\lambda\Delta x}{2}\right]\cos\frac{\lambda\Delta x}{2}\right) \qquad \textbf{(2-22)}$$

The solution for regions away from the load is:

$$w = -\frac{K}{2}\left(exp\left[-\lambda\Delta x\,(c+\varepsilon)\right]\cos\lambda\Delta xc - exp\left[-\lambda\Delta x\,(c-\varepsilon)\right]\cos\lambda\Delta xc\right) \qquad \textbf{(2-23)}$$

In (2-22) and (2-23)

$$K = \frac{\rho_{crust} - \rho_{air}}{\rho_m - \rho_{air}} \qquad \textbf{(2-24)}$$

and

$$\lambda = \left[\frac{(\rho_m - \rho_{air})\, g}{4D}\right]^{\frac{1}{4}} \qquad \text{(2-25)}$$

where λ defines the restoring force caused by subsidence of the crust into the asthenosphere. In (2-25) we assume that ρ_{air} is zero.

Equations (2-22) through (2-25) are incorporated in Program 1 on the accompanying diskette. Program 1 is a FORTRAN routine for calculating flexural and isostatic adjustments of a continuous elastic plate subject to arbitrary loads. Subroutine INITIALIZE specifies the initial values of parameters used in the solution, and subroutine UNITLOAD evaluates Green's function for a particular load element width and flexural rigidity. Subroutine CONVOLVE incorporates loads of different heights and densities according to concepts shown schematically in Figure 2-7. The width of each load element is constant for all elements in CONVOLVE, but the magnitude of the width depends on the scale of the region being investigated. Determining the Green's function and convolving are the heart of the algorithm. The other subroutines in Program 1 provide input and output.

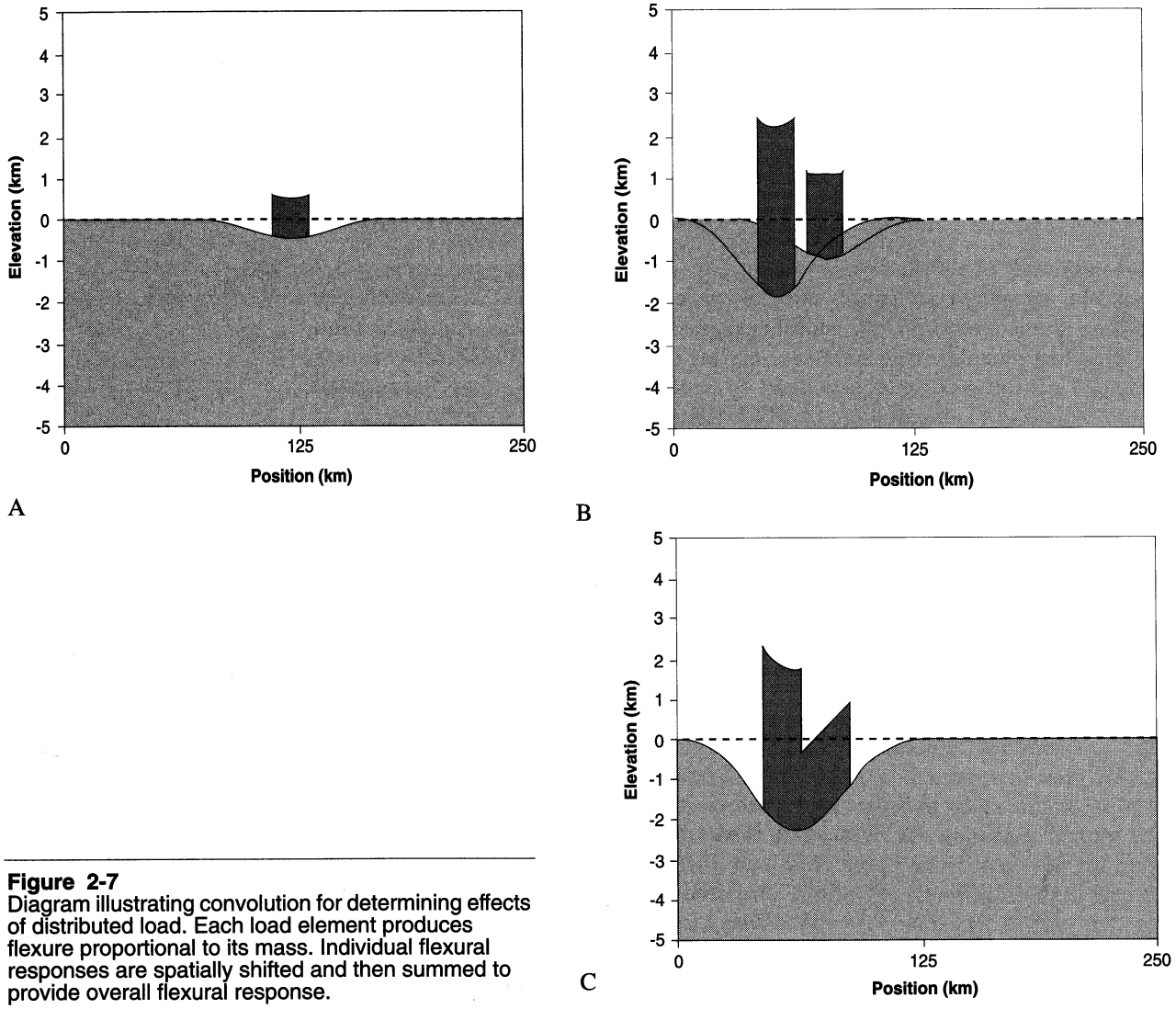

Figure 2-7
Diagram illustrating convolution for determining effects of distributed load. Each load element produces flexure proportional to its mass. Individual flexural responses are spatially shifted and then summed to provide overall flexural response.

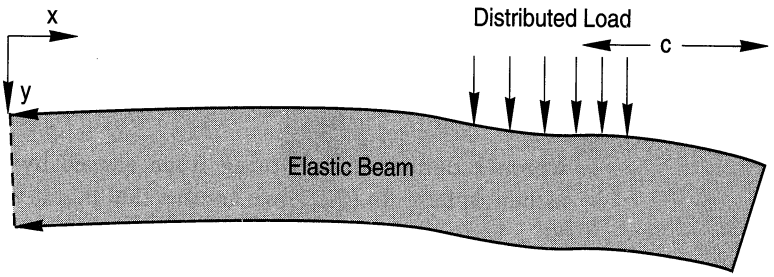

Figure 2-8 Diagram showing incorporation of distributed load in broken-plate formulation. Parameters that describe position of each load element are indicated.

Broken-Plate Flexure

Evaluating flexural response to a broken plate is more complicated than for a continuous plate. For a continuous plate, the location of the load relative to boundaries does not matter because there are no ends or boundaries to the plate. For a broken plate, the location of the load relative to the plate end, or to a break in the plate, is critical, requiring modification of the general approach and the equations. The solution for a flexed broken plate should reduce to the solution for a continuous plate when the load is sufficiently distant from the plate end. Figure 2-8 shows the configuration of the plate and load for a simple distributed load on a broken plate. The solution is given by:

$$w = \frac{\lambda K}{2} exp\,(-\lambda x)\,(\cos\lambda x + \sin\lambda x) + \lambda K exp\,[-\lambda\,(x+c)\,]\,exp\,(-\lambda c)\,(A - B + C) \qquad \textbf{(2-26)}$$

where:

$$A = \cos\lambda c \cos\lambda\,(x+c)$$

$$B = \frac{1}{2}\,[\,(\sin\lambda c - \cos\lambda c)\cos\lambda\,(x+c)\,]$$

$$C = \frac{1}{2}\,[\,(\sin\lambda c - \cos\lambda c)\sin\lambda\,(x+c)\,]$$

Because the solution depends on the position of the load, we must explicitly incorporate load position in the solution. This is accomplished in Program 2, a slightly modified version of Program 1. The general sequence of steps in the programs is similar, but for broken-plate flexure subroutines UNITLOAD and CONVOLVE in Program 1 are replaced by subroutine SEMI_INFINITE_BEAM in Program 2.

Using Programs 1 and 2

For input of flexural parameters and load configurations, Programs 1 and 2 provide an interface module, subroutine INPUT, that generates a data file for subsequent use. Alternatively, an input data file may be provided by the user. Program 1 (continuous plate) is more advanced than Program 2 (broken plate) in that it allows an initial baseline of arbitrary elevation to be specified. This permits features such as loading on the edge of a continent to be represented by incorporating the geometry of the continental margin. Both programs allow multiple loading events, using individual load elements of specified height and density. Program 1

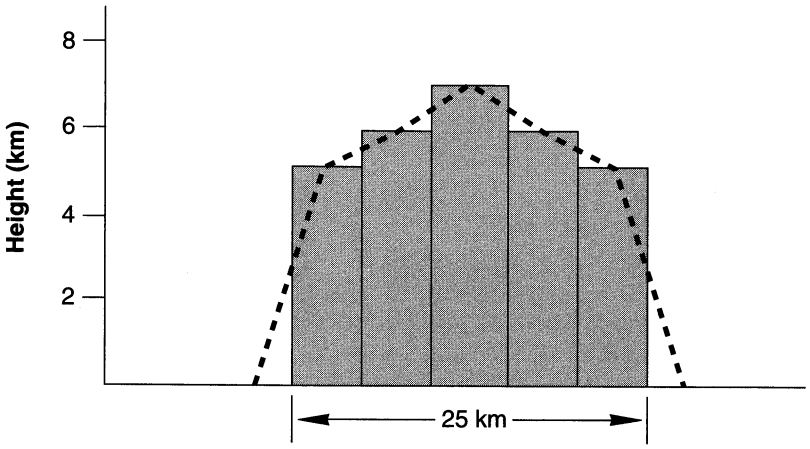

Figure 2-9 Cross section showing simple load geometry used to evaluate role of flexural rigidity in flexure. Series of rectangular loads approximate polygonal load indicated by dashed line.

also allows inclusion of hidden loads generated by density anomalies within the plate. Such features are useful for modeling rift-related basins. For a dynamic interactive model, where mass is redistributed by erosion and deposition, Programs 1 and 2 must be coupled with programs discussed in subsequent chapters. An example is provided in Chapter 7, where Program 1 is linked with sediment-transport programs to produce Program 25.

SIMULATION OF LITHOSPHERIC FLEXURE

Here we use Program 1 and Program 2 to treat simple problems involving lithospheric flexure. Through examples, we explore the nature of flexure and variations in flexural response to boundary conditions, flexural parameters, and load geometry. Initial examples provide insight into lithospheric flexure and its sensitivity to different parameters. We build on these examples to investigate responses of simple mountain-basin system under different assumptions of basin evolution.

Experiment 2-1: Flexural Rigidity

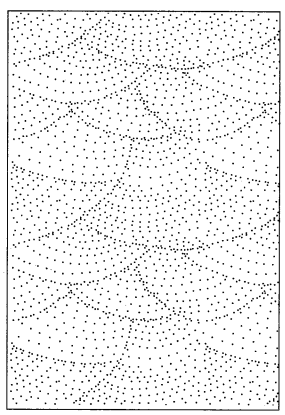

In Experiment 2-1 we simulate response of the lithosphere to simple loads. Most of the simulations use the equivalent of a polygonal load. A polygonal load can be approximated by a series of narrow rectangles as shown in Figure 2-9, where each load element is 5 km wide, with heights as specified. An example input file for Experiment 2-1 is provided in Table 2-1. The file was generated with the INPUT module in Program 2-1.

Experiment 2-1 consists of four solutions, each using a different value for flexural rigidity D. Experiment 2-1a uses the relatively low value of 1×10^{20} Newton-meters, corresponding to an equivalent elastic thickness of only 2.5 km. The resulting flexure (Figure 2-10) is significantly less than under simple isostatic assumptions, even for this relatively weak lithosphere. An important feature arising from crustal flexure is the region of positive relief called a peripheral bulge (Figure 2-10). The magnitude of the peripheral bulge is significantly less than the maximum deflection beneath the load, and often will be a subtle feature in actual basins. As flexural rigidity increases (Experiment 2-1b and c), the flexural deflection and associated peripheral bulge decrease, but the width of the flexure

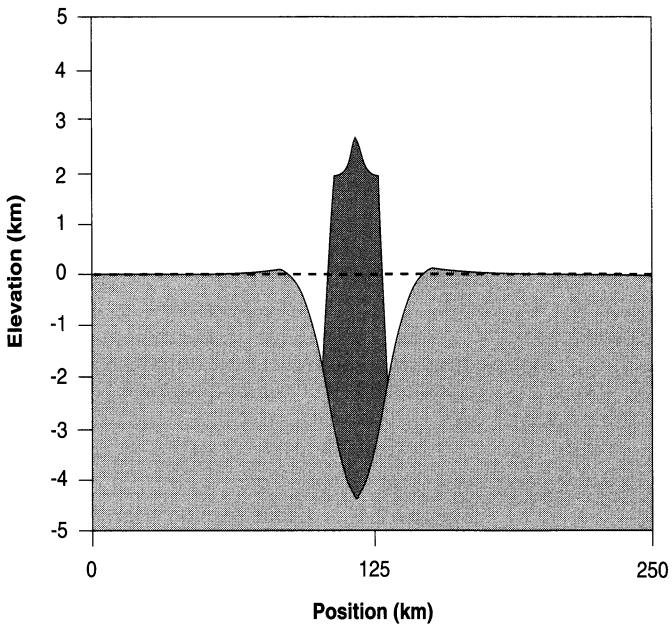

A

Figure 2-10
Cross sections showing flexural responses to load for lithospheric flexural rigidities of (A) 1 x 10^{20} Nm, (B) 1 x 10^{21} Nm, and (C) 1 x 10^{22} Nm. Positions of peripheral bulges are indicated.

Table 2-1 Input file for Experiment 2-1a

exp2-1a	**/name for this particular simulation**
0	**/ baseline flag, 0 = no baseline; nonzero number indicates number of baseline points**
1	**/number of loading events**
5000.0 0.10E+21	**/width of load elements and flexural rigidity**
5	**/number of load elements defining first loading event**
98 5000. 2700.	**/node number, height, density of load element 1**
99 6000. 2700.	**/node number, height, density of load element 2**
100 7000. 2700.	**/ etc.**
101 6000. 2700.	**/ etc.**
102 5000. 2700.	**/ etc.**

increases (Figure 2-10). In Experiment 2-1c, where the flexural rigidity is more realistic at 1 x 10^{22} Nm (equivalent to an elastic thickness of about 12 km), a flexural depression is produced that is wide enough that it could represent a developing sedimentary basin.

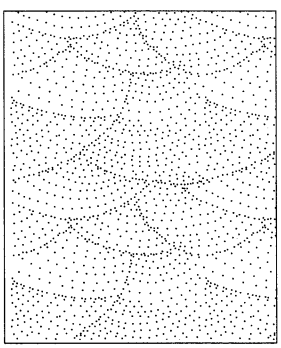

Experiment 2-2: Broken-Plate Flexure

Experiment 2-2 evaluates the differences between continuous-plate and broken-plate flexure. Two solutions investigate the effect of varying flexural rigidity (Experiment 2-2a and Experiment 2-2b), and a third solution investigates load position relative to the end of the plate (Experiment 2-2c). Table 2-2 provides the input file for Experiment 2-2a. The load is now located at the end of the plate, and there are no hidden loads. The resulting flexure for Experiment 2-2a (Figure 2-11)

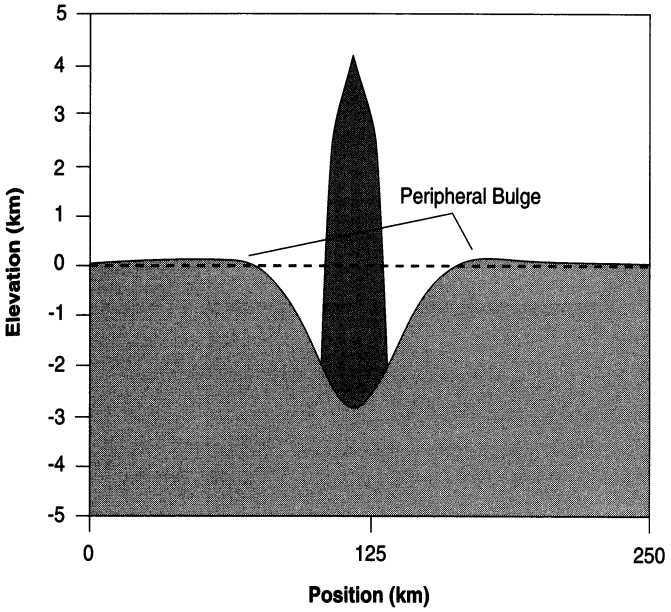

B

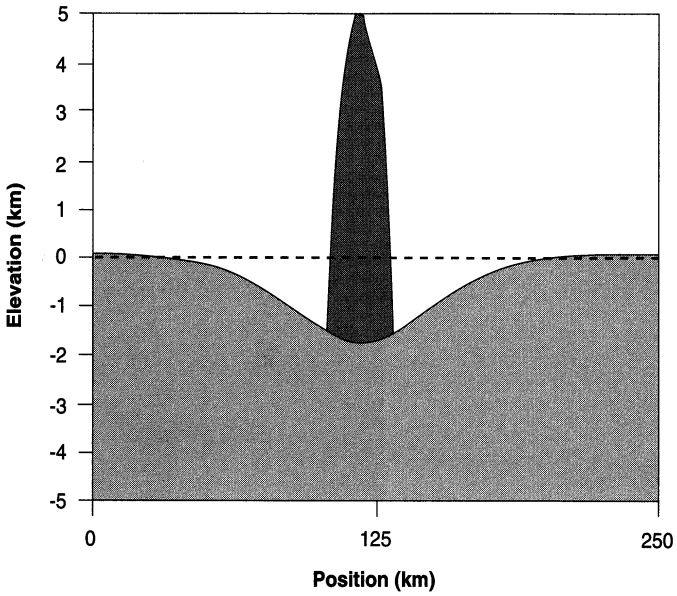

C

and Experiment 2-2b (Figure 2-12) shows greater maximum deflections, enhanced peripheral bulges, and narrower basins compared with Experiment 2-1a and Experiment 2-1b, which have corresponding flexural rigidities.

If the load is moved progressively away from the broken end of the plate, the flexure becomes increasingly similar to continuous plate flexure. Experiment 2-2c investigates the effect of a 50 km shift in load position. This shift, while relatively small for a flexural rigidity of 1 x 10^{22} Nm, dramatically changes the flexural response. Figure 2-13 shows that deflection to the right, toward the interior of the plate, is indistinguishable from continuous flexure (Figure 2-10). Deflection to the left, toward the end of the plate, however, differs substantially from continuous-plate flexure.

Table 2-2 Input file for Experiment 2-2

```
broken1a /Same entries as Table 2-1 but with no baseline flag.
1
5000.0 0.10E+22
5
1 5000. 2700.
2 6000. 2700.
3 7000. 2700.
4 6000. 2700.
5 5000. 2700.
```

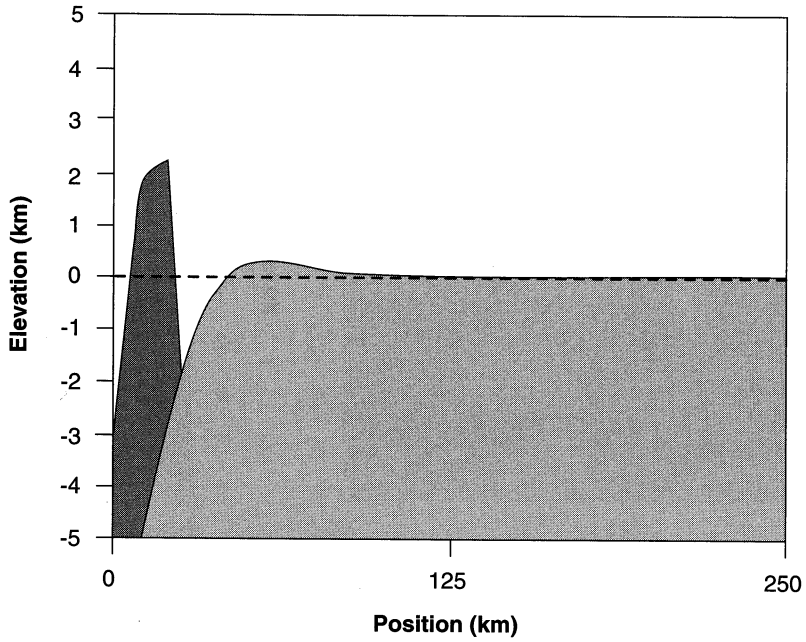

Figure 2-11 Cross section showing results of Experiment 2-2a for broken-plate flexure with test load and flexural rigidity of 1 x 10^{21} Nm. Load is placed at end of plate.

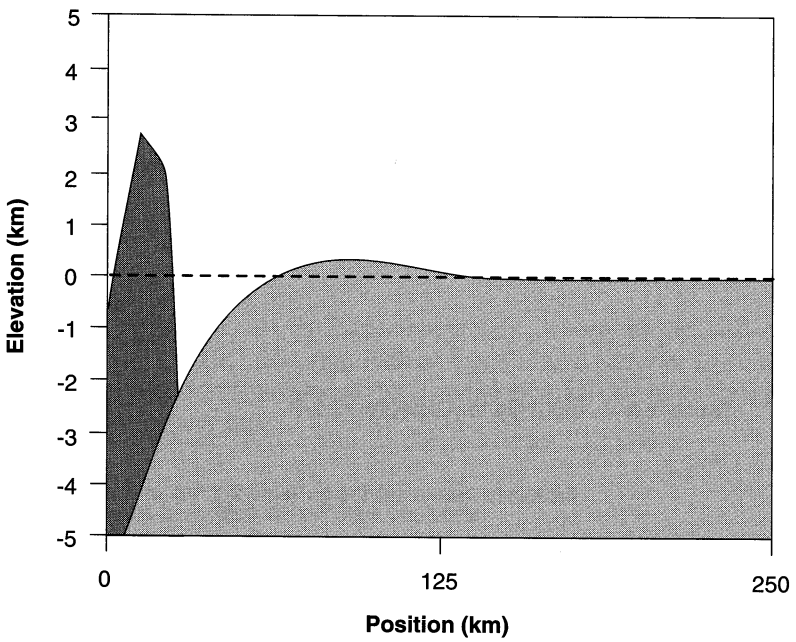

Figure 2-12 Cross section showing results of Experiment 2-2b for broken-plate flexure with test load and flexural rigidity of 1 x 10^{22} Nm. Load is placed at end of plate.

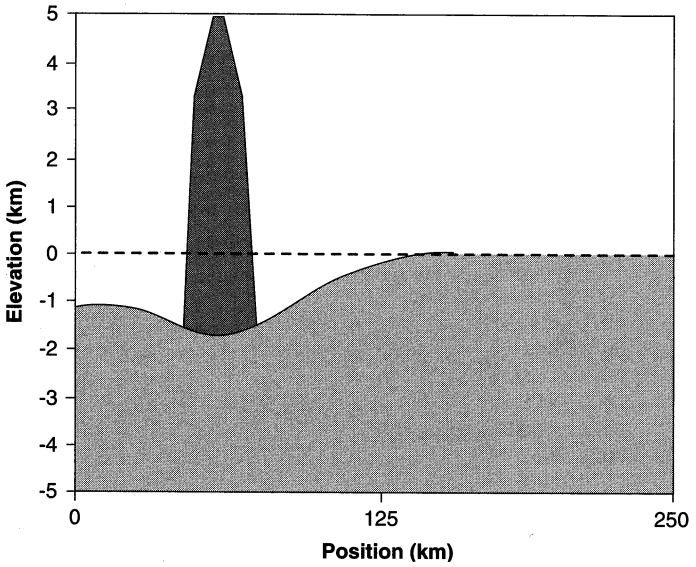

Figure 2-13 Cross section showing results of Experiment 2-2c for broken-plate flexure with test load and flexural rigidity of 1×10^{22} N m. Load is placed 50 km further inboard.

Experiment 2-3: Source and Basin Evolution

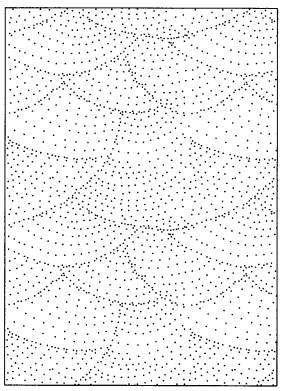

In Experiment 2-3 we evaluate the evolution of a source and basin system under simplified conditions. By source and basin system, we mean a load and its adjacent basin where the load is a feature of positive relief capable of supplying sediment to the basin. For the load we use a simple mountain range with geometry shown in Figure 2-14. The initial solution (Experiment 2-3a; Figure 2-15) shows the effect of the mountain load. Next, the resulting basin is filled with water (Experiment 2-3b) and then with sediment (Experiment 2-3c and Experiment 2-3d; Figure 2-16 and Figure 2-17). In these solutions, the sediment that fills the basin is derived externally from the mountain range. While unrealistic, it allows us to explore details of the developing basin. Finally, we examine how the basin geometry differs when the basin-filling sediment is derived from the mountain range (Experiment 2-3e; Figure 2-18).

Experiment 2-3 provides examples of forward modeling where we assume the initial shape of the mountain load and then follow the basin's evolution forward through time. The resulting model is a simplified version of the coupled model described in Chapter 7 (Program 25). In Experiment 2-3, we treat the basin development as a set of discrete events. First, the mountain load is emplaced; second, water fills the resulting accommodation space; and third, sediment fills the basin. At each step, the geometry of the basin changes. Later we will discuss ways in which the inverse solution can be determined, involving determination of the load that produced an observed sedimentary sequence.

The simple triangular load in Figure 2-14 produces the flexure shown in Figure 2-15 (input data in Table 2-3). Our choice of 1×10^{23} Nm for the flexural rigidity corresponds to an elastic thickness of approximately 25 km. The resulting basin is about 90 km wide at zero elevation. If the depression generated by the

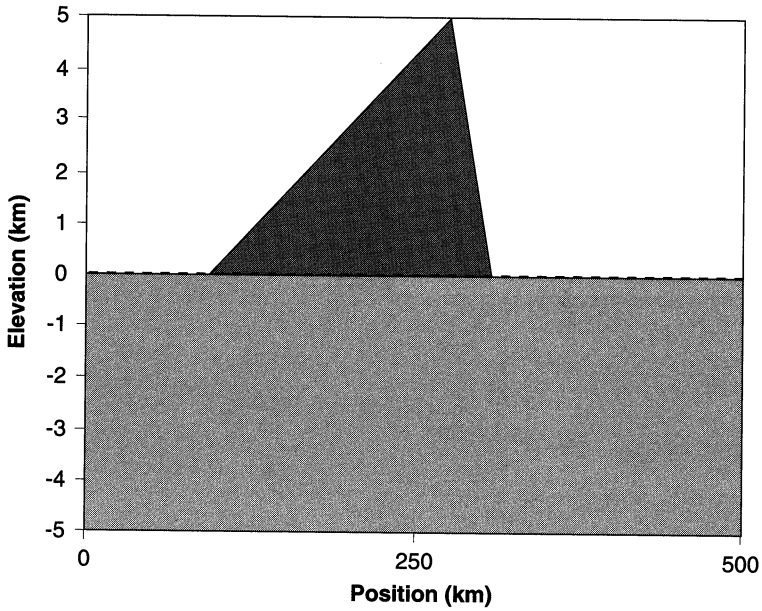

Figure 2-14 Cross section for Experiment 2-3. Wedge-shaped mountain serves as initial load that subsequently generates accommodation space.

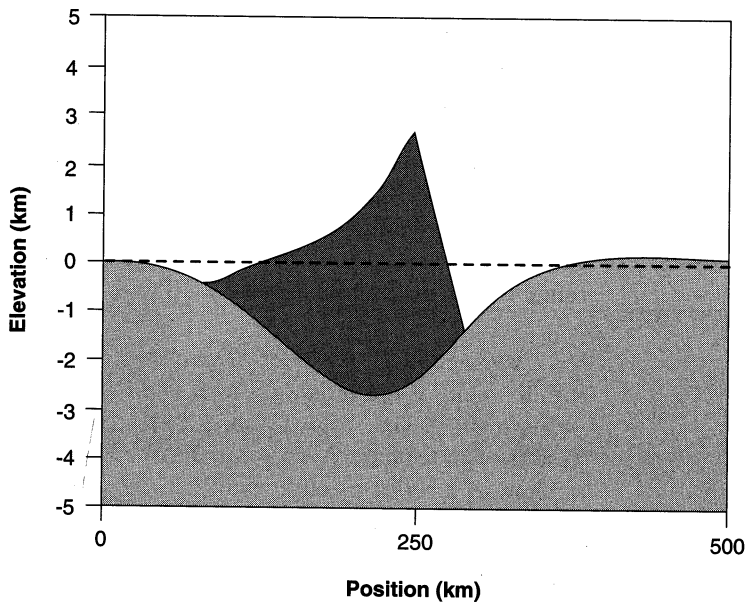

Figure 2-15 Cross section computed in Experiment 2-3a, showing basin formation without basin fill where $D = 1 \times 10^{23}$ Nm.

Table 2-3
Input file for Experiment 2-3a.

```
EXP2.3a
0
1
10000.0 0.10E+24
20
85 200. 2700.
86 500. 2700.
87 800. 2700.
88 1100. 2700.
89 1400. 2700.
90 1700. 2700.
91 2000. 2700.
92 2300. 2700.
93 2600. 2700.
94 2900. 2700.
95 3200. 2700.
96 3500. 2700.
97 3800. 2700.
98 4100. 2700.
99 4400. 2700.
100 4700. 2700.
101 5000. 2700.
102 3800. 2700.
103 2600. 2700.
104 1400. 2700.
0
```

Table 2-4
Input file for Experiment 2-3b.

```
EXP2.3b
0
2
10000.0 0.10E+24
20
85 200. 2700.
86 500. 2700.
87 800. 2700.
88 1100. 2700.
89 1400. 2700.
90 1700. 2700.
91 2000. 2700.
92 2300. 2700.
93 2600. 2700.
94 2900. 2700.
95 3200. 2700.
96 3500. 2700.
97 3800. 2700.
98 4100. 2700.
99 4400. 2700.
100 4700. 2700.
101 5000. 2700.
102 3800. 2700.
103 2600. 2700.
104 1400. 2700.
11
104 140. 1000.
105 1400. 1000.
106 1150. 1000.
107 900. 1000.
108 700. 1000.
109 505. 1000.
110 350. 1000.
111 225. 1000.
112 120. 1000.
113 42. 1000.
114 5. 1000.
0
```

flexure is filled with water (Experiment 2-3b using input file in Table 2-4), which is equivalent to adding a thickness of water comparable to the depression generated by the mountain load, the basin is modified in two ways. First, water is an additional load and causes additional subsidence. As a result, the water does not completely fill the modified basin and its surface is about 200 meters below the basin top. Second, the load of water causes the basin to become 10 to 20 km broader because the load on the crust is broader.

The effect of filling the basin with sediment (Experiment 2-3c) is similar to filling with water but is greater because the density of sediment is greater. To investigate the effect of increased density, the input file of Table 2-4 was modified to replace the density of water with that of sediment (2200 kg m^{-3}). While not filling the basin, it nevertheless allows us to investigate the effect of the sediment load. Results are shown in Figure 2-16. The basin remains unfilled by as much as

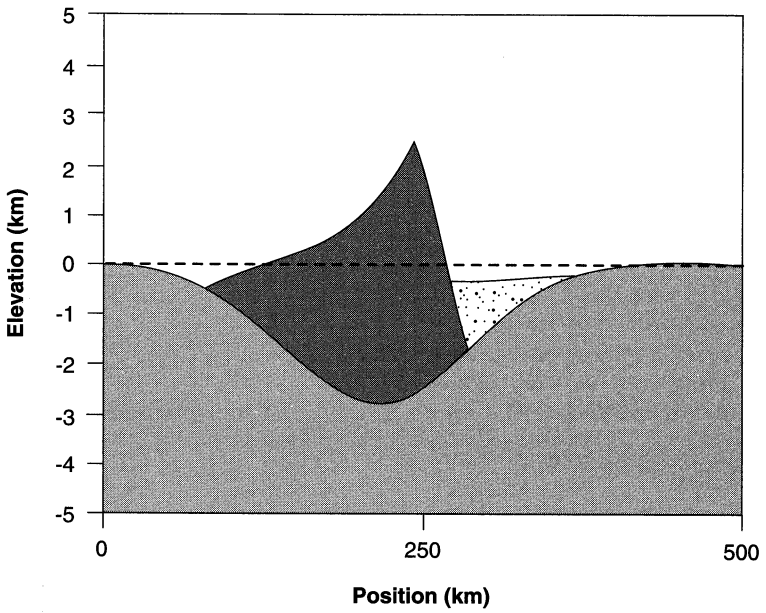

Figure 2-16
Cross section showing basin evolution modified by inclusion of sediment in Experiment 2-3c.

345 meters vertically, and the maximum peripheral bulge has less amplitude and has migrated 20 km farther from the mountain front.

The basin can be filled completely with sediment by an iterative scheme where additional loads are added successively to fill the remaining accommodation space until the basin is filled to a specified level. In Experiment 2-3d, several such iterative steps fill the basin with sediments, but we also allow an additional load of about 100 meters of water above the final sediment pile. The input file for Experiment 2-3d is in Table 2-5 and results are shown in Figure 2-17. The final basin is about 50 km wider than the initial depression, and at its deepest point (away from the mountain load), it is more than 400 meters deeper than the initial accommodation space generated from the mountain load.

Here we should reconsider the issue of isostatic versus flexural response of the lithosphere to applied loads. In Experiment 2-3d the net effect of emplacing a mountain and sediment load allowed a basin to form that is more than 1600 meters deep, with 100 meters of water in addition. We can now do a "thought exercise" in which this 1600-meter-thick sequence at node 105 in Experiment 2-3 has been estimated from measured sections or borehole data and we wish to back calculate the tectonic subsidence in the absence of loads of sediment and water. Assuming isostatic compensation [Equation (2-3)], 1600 meters of sediment plus 100 meters of water should cause about 1100 meters of subsidence at node 105. That is to say, if we removed the sediment and water, we would expect 1100 meters of rebound, moving the basin floor to 600 meters below the zero datum. Therefore, our estimate of tectonic subsidence at node 105 would be 600 meters. However, we know the tectonic subsidence at node 105 because it is the subsidence generated at that point by the initial loading of the mountain system, as obtained in Experiment 2-3a (Figure 2-15). The actual deflection at node 105 is about 1375 meters. If we assumed only isostasy in our analysis, we would have significantly underesti-

Table 2-5
Input file for Experiment 2-3d.

```
EXP2.3d
 0
 3
 10000.0 0.10E+24
 20
 85 200. 2700.
 86 500. 2700.
 87 800. 2700.
 88 1100. 2700.
 89 1400. 2700.
 90 1700. 2700.
 91 2000. 2700.
 92 2300. 2700.
 93 2600. 2700.
 94 2900. 2700.
 95 3200. 2700.
 96 3500. 2700.
 97 3800. 2700.
 98 4100. 2700.
 99 4400. 2700.
 100 4700. 2700.
 101 5000. 2700.
 102 3800. 2700.
 103 2600. 2700.
 104 1400. 2700.
 12
 104 485. 2200.
 105 1647. 2200.
 106 1409. 2200.
 107 1179. 2200.
 108 963. 2200.
 109 765. 2200.
 110 590. 2200.
 111 436. 2200.
 112 307. 2200.
 113 199. 2200.
 114 113. 2200.
 115 46. 2200.
 13
 104 100. 1000.
 105 100. 1000.
 106 100. 1000.
 107 100. 1000.
 108 100. 1000.
 109 100. 1000.
 110 100. 1000.
 111 100. 1000.
 112 100. 1000.
 113 100. 1000.
 114 100. 1000.
 115 100. 1000.
 116 50. 1000.
 0
```

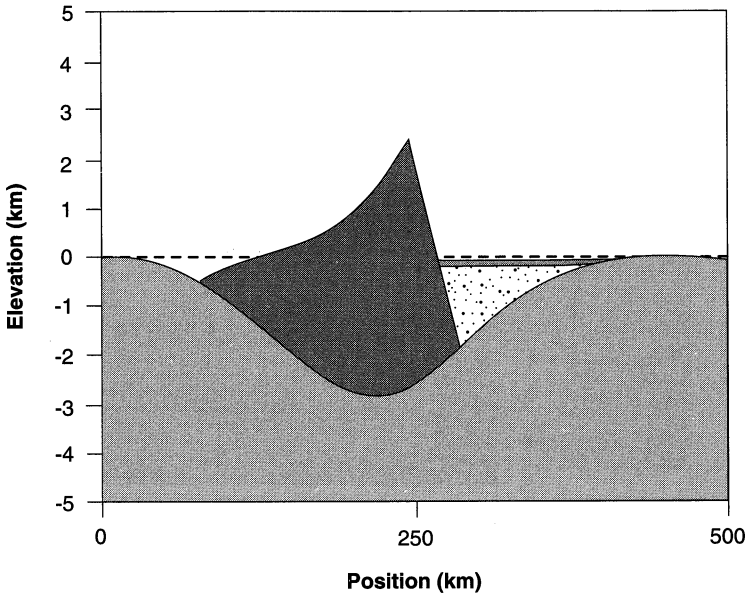

Figure 2-17
Cross section computed in Experiment 2-3d of final basin geometry, including sediment plus 100 meters of water. Geometry shown is obtained with successive iterations. Node 105 in Table 2-5 corresponds to 300 km on x-axis.

mated the backstripped depth of the basin, and entirely missed the importance of the adjacent mountain load in producing the basin. Because of the flexural strength of the lithosphere and the finite extent of the load, the load of sediment plus water produced only about 400 meters of subsidence. Most of the accommodation space produced is the result of the emplacement of the mountain system.

Thus far we have produced a coupled mountain-and-basin system that is in flexural equilibrium, given that the initial load is not eroded and the source for basin sediment is external. In Experiment 2-3e, material removed from the mountain load fills the basin. Two-thirds of the material is deposited in the basin, with the remaining one-third assumed to bypass the basin as the products of chemical weathering. The results are shown in Figure 2-18, with input file in Table 2-6. Although we have removed as much as 1200 meters from parts of the mountain load, rebound of the underlying lithosphere causes the final topography to be reduced by about 750 meters compared with our previous uneroded model (Experiment 2-3d). Also, removal of load from the mountain produces less accommodation space for sediment. As a result, material that was below the datum in Experiment 2-3d is now above the datum (although it may not erode, as it is below the elevation of the peripheral bulge).

Finally, we wish to evaluate the flexural response to a distributed load such as a mountain system if the plate is broken rather than continuous. Figure 2-19 shows the results of applying the same load to a broken plate. As noted before, the closer the load is to the end of the plate, the greater the difference between the broken-plate and continuous-plate flexure models. Because the load is reasonably wide (about 200 km), the flexural response on the side away from the broken end is nearly indistinguishable from the continuous-plate flexure. This is important because it allows us to use the simpler continuous-plate model even if the plate

Table 2-6
Input file
for Experiment 2-3e.

```
EXP2.3e
0
2
10000.0 0.10E+24
20
85 200. 2700.
86 500. 2700.
87 800. 2700.
88 1100. 2700.
89 1400. 2700.
90 1700. 2700.
91 2000. 2700.
92 2300. 2700.
93 2450. 2700.
94 2650. 2700.
95 2700. 2700.
96 3000. 2700.
97 3150. 2700.
98 3350. 2700.
99 3500. 2700.
100 3800. 2700.
101 3800. 2700.
102 2800. 2700.
103 1600. 2700.
104 1000. 2700.
13
103 250. 2200.
104 635. 2200.
105 1547. 2200.
106 1359. 2200.
107 1179. 2200.
108 963. 2200.
109 765. 2200.
110 590. 2200.
111 436. 2200.
112 307. 2200.
113 199. 2200.
114 113. 2200.
115 46. 2200.
0
```

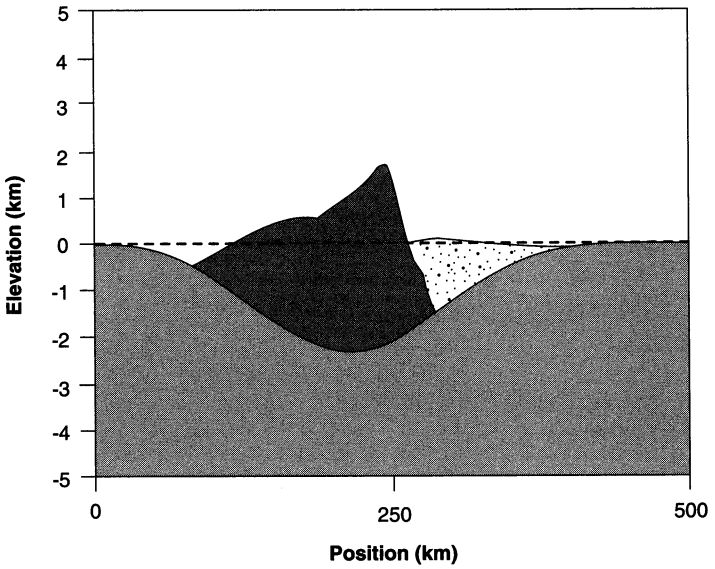

Figure 2-18
Cross section showing results of Experiment 2-3e, which assumes sediment that fills basin is derived from mountain load. Redistribution of sediment changes shape of basin.

contains a break, provided that the basin of interest is far inboard of the break, as for example where terrane is thrust upon the edge of a plate.

An Inverse Approach

The models just described move forward in time and therefore fit naturally with the basin-filling models of subsequent chapters. Given the temporal evolution of a load, the models predict the temporal evolution of a basin. But often the geologic questions to be answered require the inverse approach. The temporal evolution of the basin is known from the geometry and characteristics of the basin fill, and we want to determine the temporal evolution of the load. To accomplish this we reverse the order of steps in Experiment 2-3. The basin fill is placed on the crust first and flexure calculated. The fill will rise above the baseline because it is impossible for a pile of sediment to create exactly the correct amount of accomodation space. By trial-and-error we try different loading scenarios until the coupled load-basin system produces an evolution consistent with its sedimentary history.

RIFTING, CRUSTAL THINNING, AND HIDDEN LOADS

Basins are not created solely by thickening of crust. Thinning of crust during rifting and extension causes flexure and also creates accommodation space, as illustrated in Figure 2-20, where flexure is caused by mantle material replacing crustal material in the lithospheric column within the region of extension. The load is simply the product of the volume of replaced material times the density difference between crust and upper mantle. This load is internal to the plate and hidden from view, but its effects are similar to those obtained by applying an excess mass to the top of the plate, except that it occupies none of the region created by the flexure.

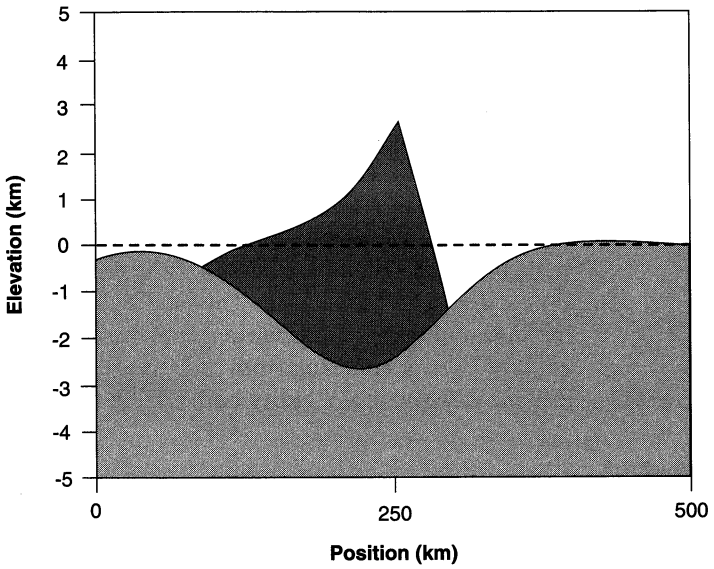

Figure 2-19 Computed cross section of foreland basin resulting from mountain load on a broken plate. Resulting foreland basin closely resembles that developed in continuous-plate model.

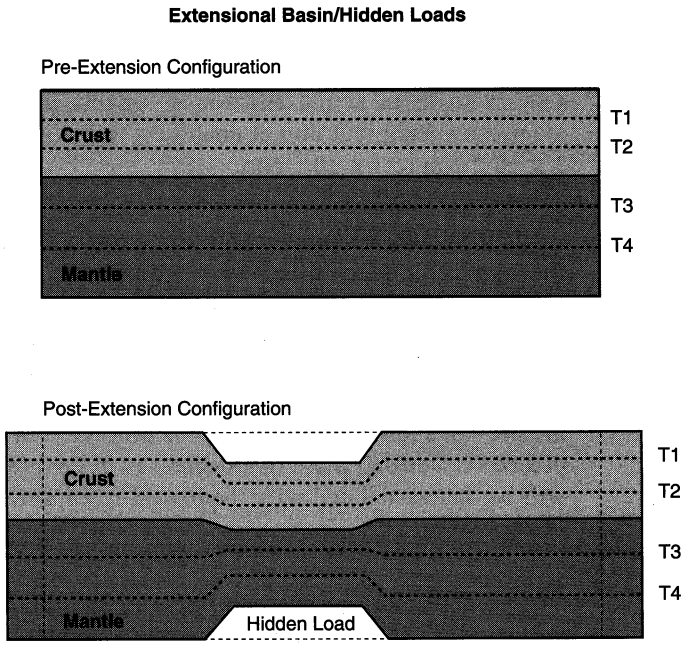

Figure 2-20 Geometry in which extension of crust produces hidden load. Crustal thinning causes crustal rock to be replaced by underlying mantle rock. Extension may cause disruption of lithospheric isotherms (T1 to T4) which will lead to additional transient subsidence.

Program 1 allows hidden loads to be incorporated via subroutine HIDDEN. We assume that the load replaces crustal material, but because it is the density difference computed by subroutine HIDDEN that is ultimately convolved with the Green's function, we may assume any composition for the hidden load.

In analyzing a region where rifting or lateral extension of the crust has occurred, it is important to consider the distribution of temperatures in the lithosphere and the effect on flexure. If lithospheric material is brought rapidly closer to the surface during extension, depth to a particular isotherm decreases (Figure 2-20). When rifting stops the lithosphere cools, but cooling may take tens of millions of years. Consequently, the strength and flexural rigidity of the plate decrease during rifting. This decrease is well documented by backstripping studies along rifted continental margins. As the plate cools following rifting, it increases in density, causing both a decrease in volume through thermal contraction and an additional load. This additional load acts on a stronger plate than did the initial hidden load because a cooler plate is more flexurally rigid. Next we will explore flexure resulting from hidden loads associated with rifting. In Experiment 2-4 we vary flexural rigidity both during and following rifting.

Experiment 2-4: Hidden Loads and Response to Rifting

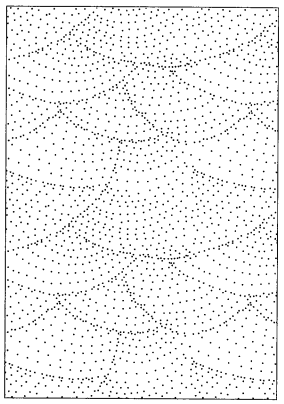

Experiment 2-4 simulates the flexural response of a plate to a narrow rift, with particular attention to the controls on the width of the basin produced. The geometry of a load is shown in Figure 2-20, with the crust thinned by 20 km over a region that is 25 km wide. Within this region the mantle is assumed to possess a density of 3200 kg m^{-3}, a value slightly less than the lithospheric mantle density that represents partial inclusion of asthenospheric material and higher temperatures of the plate during rifting. The assumed flexural rigidity helps control the initial subsidence. In Figure 2-21, flexure resulting from a hidden load is shown for four values of flexural rigidity. The lowest value (1 x 10^{14} Nm) produces an isostatic response, while the higher values produce different patterns of flexure. Observations in actual rift zones suggest low values of rigidity during initial stages of rifting, but do not enable us to distinguish among values in the range of 1 x 10^{14} Nm to 1 x 10^{19} Nm.

Rifting may occur over short time intervals, precluding development of basins that are completely filled with sediment at all times. A typical response may involve deposition of sediment both during and after rifting, with sediment forming a load on a cooling and therefore increasingly rigid plate. The final response to emplacement of any load is given by the response of the weakest plate that exists during or after the loading. If the rigidity of the plate increases, the effect of the previous low flexural rigidity is preserved in the record. However, if loads are placed on a strong plate that decreases in flexural rigidity, the preserved response will be that associated with the lowest flexural rigidity, and evidence of the initial flexure is lost.

Table 2-7
Input file for Experiment 2-4.

```
hidden1
4
97 0.
98 -2424.
102 -2424.
103 0.
1
5000.0 0.10E+23
5
98 2424. 2200.
99 2424. 2200.
100 2424. 2200.
101 2424. 2200.
102 2424. 2200.
5
98 20000. 2900.
99 20000. 2900.
100 20000. 2900.
101 20000. 2900.
102 20000. 2900.
```

Modeling the combined effects of crustal thinning, subsequent cooling, and sediment loading is accomplished by the input data listed in Table 2-7. Initial subsidence is simulated through a baseline function. The baseline is defined by four points in Table 2-7. The effect of sediment fill is simulated by an external load at five nodes. Additional cooling and densification is simulated as a hidden load. The response of the lithosphere to cooling and sediment deposition after rifting is shown in Figure 2-22. If the lithosphere cools sufficiently so that the additional loads (both hidden and sedimentary) act on a plate with rigidity of 1 x 10^{22} Nm, a depression forms that is broader than the initial rift geometry. If, however, the cooling lithosphere and sediment load a weaker lithosphere with a rigidity of 1 x 10^{20} Nm, the basin geometry is quite different. An evolving rift basin may

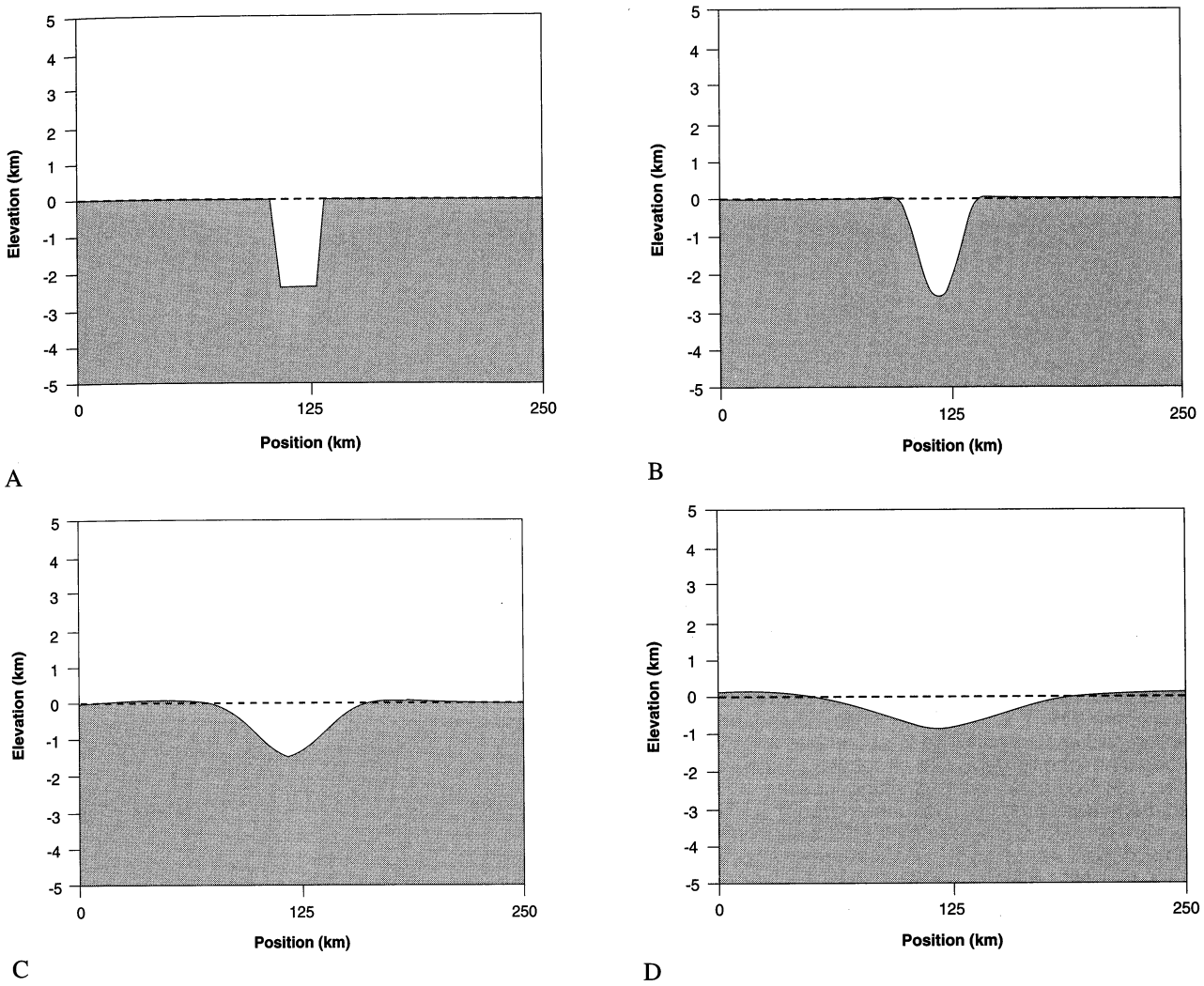

Figure 2-21 Cross sections computed in Experiment 2-4 showing flexural response to hidden loads for flexural rigidities of (A) 1 x 10^{14} Nm, (B) 1 x 10^{19} Nm, (C) 1 x 10^{21} Nm, and (D) 1 x 10^{22} Nm, that span transition from isostatic to flexural response.

include evidence of pseudo-isostatic response, with low and intermediate flexural rigidity, yielding a complex basin geometry and involved depositional history.

CRYPTIC LITHOSPHERIC LOADING

Not all tectonic processes that produce or increase accommodation space are as readily recognizable as the loads described above, and for this reason they are called cryptic loads. Horizontal compression acting on a plate is one example of a cryptic load. Until now, we have neglected horizontal compression in (2-21) because it causes only a small increase in the deflection. But Cloetingh and others (1989) argue that in some cases this small deflection may create geologically significant accommodation space. Another type of cryptic load may be caused by mantle flow. Gurnis(1993) has argued that subduction and mantle flow induced by descent of a subducted slab can produce a depression along a continental margin.

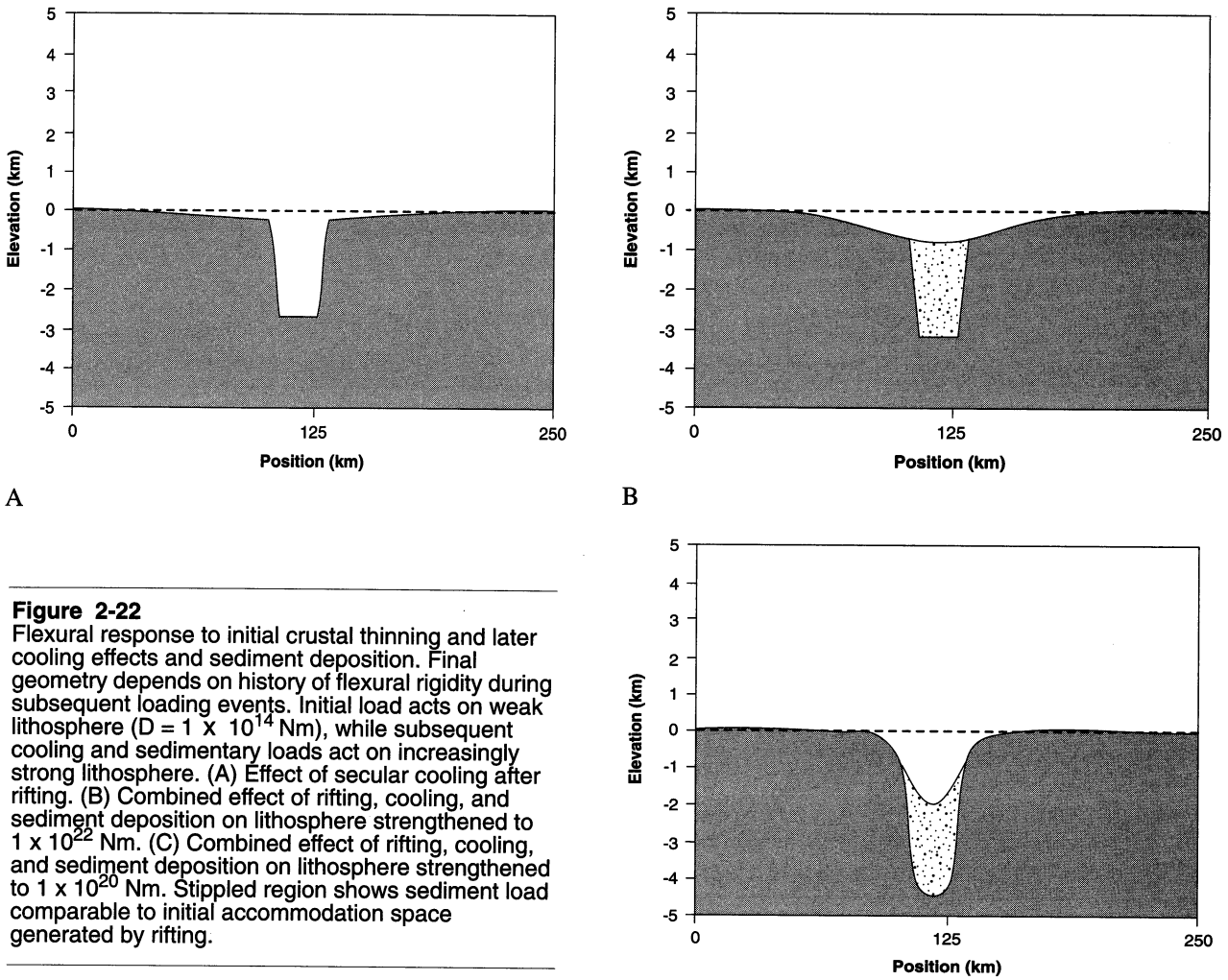

Figure 2-22
Flexural response to initial crustal thinning and later cooling effects and sediment deposition. Final geometry depends on history of flexural rigidity during subsequent loading events. Initial load acts on weak lithosphere ($D = 1 \times 10^{14}$ Nm), while subsequent cooling and sedimentary loads act on increasingly strong lithosphere. (A) Effect of secular cooling after rifting. (B) Combined effect of rifting, cooling, and sediment deposition on lithosphere strengthened to 1×10^{22} Nm. (C) Combined effect of rifting, cooling, and sediment deposition on lithosphere strengthened to 1×10^{20} Nm. Stippled region shows sediment load comparable to initial accommodation space generated by rifting.

We call these cryptic loads because it is very difficult to determine when they are important and how large their effects might be. For example, isostatic backstripping a flexural environment produces artifacts that could be erroneously linked to cryptic processes.

PRESERVATION OF SEDIMENTARY BASINS

Thus far we have ignored basin preservation. We have shown that it is generally necessary to load the lithosphere to produce accommodation space. If the mass that initially produced the accommodation space is removed, then the basin should rebound and eventually disappear. The long-term existence of a basin suggests that loads either must be preserved or the processes that created the basin must change to preserve it.

Maintaining a Load

There are several ways in which the load producing a basin can be preserved. The simplest way is the addition of a permanent hidden load such as occurs in exten-

sional basins. Only major changes in crustal temperature or subsequent tectonic events are likely to modify the hidden load.

Of more interest is how basins formed by supracrustal loading, such as foreland basins associated with thrust belts, are preserved. The history of a foreland basin involving a simple overthrust geometry is shown schematically in Figure 1-8. When the thrust or mountain load erodes, the basin and load rebound, eventually leading to complete removal of both the basin and load (Figure 2-23). In this light, it is surprising that basins such as the Taconic and Acadian Appalachian basins of Pennsylvania remain, even though there is no obvious topographically high load to maintain them. The explanation is that loads associated with the Taconic and Acadian orogenic events were emplaced at least partly on the continental margin of North America. Therefore the baseline that controls erosion, sea level, is substantially above the baseline on which the load sits, namely the continental margin. As shown schematically in Figure 2-24, such a situation allows preservation of a significant fraction of a basin even when the load has eroded to near sea level. In the Taconic and Acadian basins, there may be as much as 10 to 20 km of Appalachian load beneath the coastal plain of the mid-Atlantic region.

"Pocket" or small basins may be preserved differently. If the lithosphere strengthens during deposition of sediment and before erosion of the initial load,

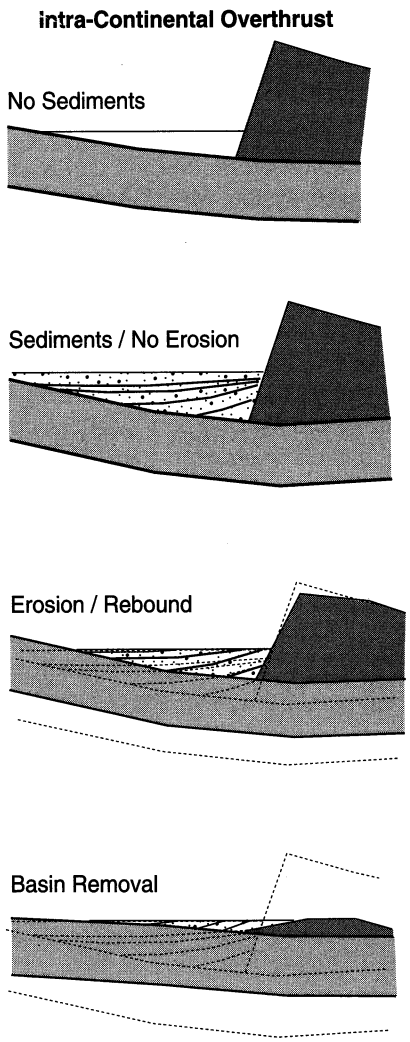

Figure 2-23
History of foreland basin system involving intra-continental overthrusting where load is emplaced at base level. Basin is eroded completely when load is eroded.

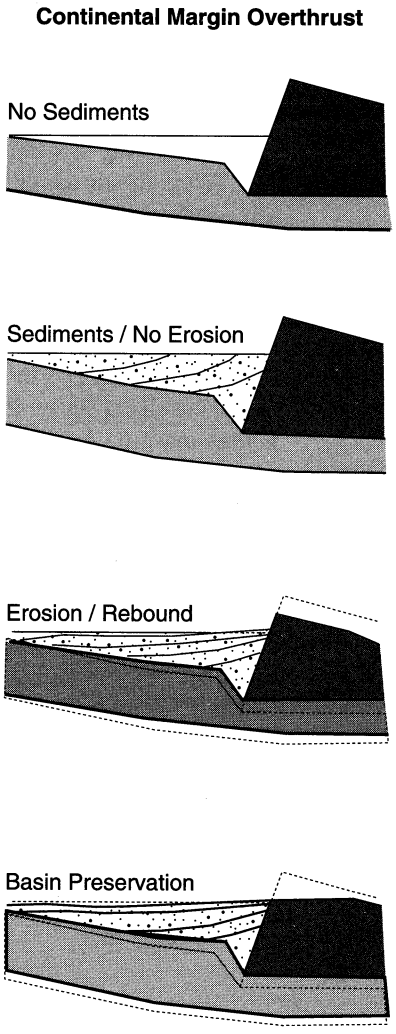

Figure 2-24
History of foreland basin system when load is emplaced below baseline, as would happen along a continental margin. In this case, basin may be preserved even after reduction of mountain topography to sea level.

then the flexural geometry will change. A narrow deep basin on weak lithosphere will rebound over a broader region. Such a situation will preserve much of the original basin.

Rates of Crustal Rebound

Supracrustal loads eventually will be eroded and basins will rebound. The rate at which rebound occurs is controlled by the rate of viscous flow in the lower crust and upper mantle and the rate of erosion and redistribution of loads. Flow rates in the crust and mantle place limits on the maximum rate of crustal response to changing loads, while rates of erosion and redistribution of loads determine the effective rate of rebound. Erosion and redistribution of loads are treated next.